Resonance Raman scattering in GaAs-$Al_xGa_{1-x}As$ superlattices: Impurity-induced Fröhlich-interaction scattering

W. Kauschke, A. K. Sood,* M. Cardona, and K. Ploog
Max-Planck-Institut für Festkörperforschung, Heisenbergstrasse 1, D-7000 Stuttgart 80, Federal Republic of Germany
(Received 14 November 1986)

We report measurements of Raman scattering from LO phonons in resonance with quasi-two-dimensional excitons in a 104-Å GaAs–125-Å $Al_{0.25}Ga_{0.75}As$ superlattice. Incoming and outgoing resonances are observed at discrete excitons formed from first and second conduction and valence subbands. As already pointed out by Zucker *et al.*, the resonant Raman profile shows a stronger outgoing resonance as compared with the incoming one. We present a quantitative explanation of the observed asymmetry of both resonance channels by invoking the impurity-induced intraband Fröhlich scattering mechanism, an effect also observed in bulk semiconductors. This analysis differs from that of Zucker *et al.*, which was based on the details of the quantized quasi-two-dimensional excitons. We believe that the latter mechanism may explain resonance asymmetry for a special range of superlattice parameters, while the one proposed here should be more general, extending all the way to the two-dimensional case.

I. INTRODUCTION

Raman scattering from phonons in semiconductor superlattices and multiple quantum wells (MQW), in particular GaAs-$Al_xGa_{1-x}As$ systems, is being extensively studied in order to understand the nature of the vibrational modes and their interaction with electrons (or excitons).[1–3] The optical properties of such superlattices are dominated by discrete and continuum excitons formed from the confined electron-hole pairs.[4–6] These electron-hole pairs, confined in the GaAs layers of GaAs-$Al_xGa_{1-x}As$ superlattices and thus termed quasi-two-dimensional excitons, strongly affect the optical properties.[7–9]

Recent Raman experiments have shown the difference between the concepts of zone-folded vibrational modes, applicable to acousticlike phonons, and confined modes for optical phonons.[10] The LO phonons of the superlattice [with (001) growth direction and D_{2d} point group] belong either to the B_2 or the A_1 irreducible representations of D_{2d}. The A_1 modes, dipole-forbidden in bulk GaAs (diagonal Raman tensor), are dipole-allowed in the superlattice. The values of the diagonal Raman tensor components, as calculated within a polarizability model, are small and hence A_1 modes should, in general, not be observed.[11,12] It has, however, been shown that these A_1 modes resonate much more strongly than the B_2 modes, so much that only A_1 modes are seen close to resonance. This fact is analogous to the resonant enhancement of the forbidden Raman scattering by LO phonons in bulk semiconductors, arising from the intraband Fröhlich electron-phonon interaction.

Resonant Raman scattering (RRS) in GaAs-$Al_xGa_{1-x}As$ superlattices was first reported by Manuel *et al.*[13] This work was performed at room temperature. The results of Zucker *et al.*[2] on resonance enhancement at low temperature in these superlattices clearly brought out the role of quasi-two-dimensional discrete excitons. In these measurements, the resonance profile showed a peak when the exciting photon energy $\hbar\omega_L$ equaled the energy of the $n=1$, electron–heavy-hole (e-HH) exciton of GaAs (incoming resonance). In the case of the $n=2$, heavy-hole exciton, in addition to the incoming resonance, a resonance peak was observed when the scattered photon energy ($\hbar\omega_S$) matched the $n=2$ exciton (outgoing resonance). Similar incoming and outgoing resonances were observed in GaAs-AlAs superlattices at the $n=1$, e-HH exciton. The outgoing resonance is observed to be stronger than the incoming one. Zucker *et al.*[2] attributed this asymmetry between the strengths of incoming and outgoing resonances to an exciton-LO-phonon scattering process in which the exciton makes a transition to a different quantum-well state at higher energy (from $n=2$ to $n=3$). On the other hand, Sood *et al.*[10] conjectured that double resonance effects arising from the impurity-induced Fröhlich interaction scattering, analogous to those found in bulk GaAs, are the cause of the stronger outgoing resonance. A stronger incoming than outgoing resonance is observed for the resonance of Raman scattering by LO phonons with extended excitons.[14] Zucker *et al.*[14] explain the asymmetry in a way similar to Ref. 2 by the interaction of the extended exciton state with a discrete exciton at lower energy via the LO phonon. In asymmetric modulation-doped quantum-well structures Suemoto *et al.*[15,16] showed that the Raman scattering by LO phonons resonates when the scattered photon (outgoing resonance) matches the transition from the uppermost hole subband to the conduction subbands ($n \leqq 11$).

In this paper we report Raman measurements of LO phonons in a GaAs-$Al_xGa_{1-x}As$ superlattice at temperature $T \approx 2$ K in resonance with $n=1$ and $n=2$, e-HH discrete excitons. We show that the stronger outgoing resonance can be quantitatively understood on the basis of impurity-induced intraband Fröhlich scattering. Detailed

calculations are performed for the $n=2$ resonances. In this case excitonic effects should be weaker[5] and it is reasonable to treat the resonance by assuming uncorrelated electrons (two-dimensional interband minimum). The inclusion of continuum Coulomb interaction would considerably complicate the problem without adding much physical insight to it.[17]

In our model, which has been shown to work well in three dimensions,[18] we evaluate a fourth-order process in which the incident photon creates a virtual electron-hole pair, this pair is scattered by the LO phonon and then by the impurity, and finally recombines to give the scattered photon. This process, although of higher order, can dominate over the standard quadrupole-type (**q**-dependent) third-order Fröhlich mechanism[17,19] because phonons of much larger wave vector are involved: The impurities carry away the difference between this wave vector and the small optical scattering vector.

In a superlattice, or more precisely, in the multiple quantum wells treated here, two scattering mechanisms involving Fröhlich interaction are possible.[20] One of them, which involves no **q** transfer parallel to the layers, results from the different penetration of electron and hole wave functions into the barriers. We neglect this mechanism here because of the high barriers of our samples (large period) and the fact that the larger penetration depth due to the reduction in barrier height of the valence band, as compared with the conduction band, is compensated by that due to the larger mass of the heavy holes. The mechanism we actually treat involves **q** transfers parallel to the layers and, for backscattering, can only be activated by defects such as impurities or irregularities at the interface. The **q** transfer due to the defects must, however, remain below π/d_1 (d_1 = GaAs layer thickness), otherwise the LO phonons convert into their TO modes (for spherically symmetric impurity potentials).[1]

The calculations of impurity-induced Fröhlich interaction scattering by LO phonons for 2d bands yield, like the 3d case,[18,19] stronger outgoing than incoming resonances. In two dimensions the peaks are, however, better resolved than the 3d case. For 2d bands the ratio of strengths of the outgoing and the incoming resonances depends critically on the cutoff chosen for the Coulomb potentials.

II. EXPERIMENTAL DETAILS AND RESULTS

The multiple-quantum-well sample studied was grown on a (001) GaAs substrate by molecular beam epitaxy. It consisted of 100 periods of 104-Å (d_1) GaAs/125-Å (d_2) $Ga_{0.75}Al_{0.25}As$ which were not intentionally doped. As a tunable excitation source we used a cw dye laser with the dye LD 700 (Lambda Physik, Göttingen) pumped by all red lines of a Kr^+ laser (4.5 W). The dye covered the spectral range from 1.53–1.70 eV. The measurements were performed at about 2 K in a helium bath cryostat with superfluid helium. The power density on the sample was kept below 5 W/cm^2.

Figure 1 shows the resonance of the "forbidden" Raman scattering by LO phonons [$z(x,x)\bar{z}$ backscattering configuration, where $x=(1,0,0), z=(0,0,1)$] in the region of the $n=1$ and $n=2$ quasi-two-dimensional excitons.

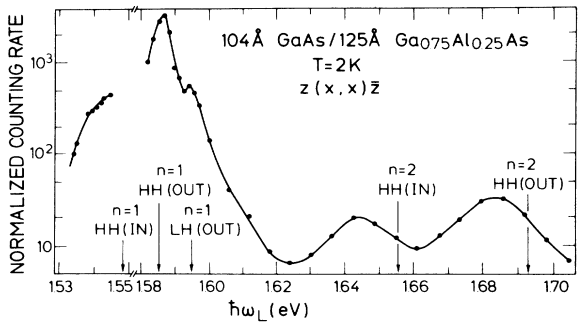

FIG. 1. Resonance profile of the forbidden scattering by LO phonons in the energy region of the $n=1$ and $n=2$ excitons. The counting rates are normalized with respect to those for single-crystal silicon without correcting for optical constants.

The counting rate has been normalized with respect to that measured for the optical phonon of Si, but the data points were not corrected for the different absorption coefficients of both materials. The line was drawn as a guide to the eye. The arrows in Fig. 1 depict the exciton levels as estimated from the calculated quantum-well levels including the exciton binding energies evaluated by Miller *et al.*[5,6] The levels are labeled by the confinement number n (starting from $n=1$) and the hole state (HH: heavy hole, LH: light hole). Incoming and outgoing resonances differ by the energy of one LO phonon ($\hbar\Omega_{LO}=36.6$ meV).

The resonance profile of the forbidden Raman scattering by LO phonons reveals the following features (Fig. 1):

(i) The *incoming* resonance at the $n=1$, electron–heavy-hole (e-HH) exciton and the *outgoing* resonances at the e-HH and e-LH excitons.

(ii) The incoming and outgoing resonances at the $n=2$, e-HH exciton. The outgoing resonance is stronger than the incoming one for the e-HH excitons. Strong luminescence near the $n=1$, e-HH exciton prevented us from completely observing the $n=1$ exciton incoming resonances.

The results are similar to those of Zucker *et al.*[2] The additional feature in our results is the observation of the $n=1$ outgoing resonances at the HH and LH excitons. The asymmetry in the strengths of the $n=2$, e-HH exciton incoming and outgoing resonances is a factor of 2, similar to that reported by Zucker *et al.*,[2] while the asymmetry of the $n=1$, e-HH exciton resonances amounts to about 6 with a large uncertainty since the structure is not completely resolved (Fig. 1). Correction for absorption would tend to increase the asymmetry, most strongly near the $n=1$ exciton (about a factor of 2) and should be less important near the $n=2$ exciton (see Ref. 8 and Fig. 15 of Ref. 9).

In the following section we will focus our attention on the well-resolved resonance near the $n=2$, e-HH exciton. We will show that intraband impurity-induced Fröhlich interaction of LO phonons with quasi-two-dimensional discrete excitons can quantitatively explain the asymmetry of the incoming and outgoing resonances.

III. THEORY AND DISCUSSION

A. Forbidden scattering by LO phonons

The q-induced (quadrupole) and surface-field-induced forbidden Raman scattering by LO phonons has been reviewed by Richter *et al.*[21] for the case of one-electron excitations at a two-dimensional critical point such as the E_1 and $E_1+\Delta_1$ gaps in III-V compound semiconductors. Their quantitative results show a symmetric enhancement of the forbidden scattering by LO phonons at the incoming ($\hbar\omega_L=E_1$) and the outgoing resonance ($\hbar\omega_L=E_1+\hbar\Omega_{\rm LO}$). In the three-dimensional case, it has been shown that ionized impurity-induced forbidden scattering yields a stronger outgoing resonance.[18,19] We will apply a formalism similar to that of Ref. 21 for the transition amplitudes and the same definition of transition matrix elements to evaluate, in fourth-order perturbation theory, the scattering efficiency of the impurity-induced Fröhlich interaction by LO phonons for 2d bands.[22] We proceed in a similar way as in the 3d case, considering uncorrelated electron-hole pairs as intermediate states.[19]

Near resonance the Raman tensor for impurity-induced scattering-$\vec{\vec{R}}_{\rm FI}$ is diagonal:

$$\vec{\vec{R}}_{\rm Fi}=\begin{pmatrix} b_{\rm Fi} & 0 & 0 \\ 0 & b_{\rm Fi} & 0 \\ 0 & 0 & b'_{\rm Fi} \end{pmatrix}, \tag{1}$$

where $b_{\rm Fi}$ and $b'_{\rm Fi}$ are Raman polarizabilities. Their difference arises from the anisotropy introduced in the cubic material by the quantum wells. At this point, we shall treat the material as three-dimensional and introduce later the two-dimensionality of the quantum well by making the mass along its axis equal to infinity (confined electronic states).

The squared Raman polarizability, proportional to the scattering efficiency ($|\hat{e}_S\cdot\vec{\vec{R}}_{\rm Fi}\cdot\hat{e}_L|^2=|b_{\rm Fi}|^2$ for $\hat{e}_S\|\hat{e}_i$), depends on the transition amplitude $W_{\rm Fi}(\mathbf{q},\mathbf{q}')$ for impurity-induced scattering by LO phonons (pseudomomentum $\hbar\mathbf{q}$, momentum transfer by the impurity $\hbar\mathbf{q}'$, f and i final and initial states)[23]:

$$|b_{\rm Fi}|^2=n_I\left[\frac{1}{\omega_L}\right]^2\left[\frac{n_S n_L}{2\pi}\right]^2\left[\frac{2M^*\Omega_{\rm LO}V_c}{\hbar^3}\right]\frac{V^3}{(2\pi)^3}$$
$$\times\int\int d^3q'\int d^3q\,|W_{fi}(\mathbf{q},\mathbf{q}')|^2$$
$$\times\delta(\mathbf{k}_L-\mathbf{k}_S-\mathbf{q}-\mathbf{q}')\,. \tag{2}$$

n_I denotes the concentration of ionized impurities, $n_{L,S}$ are the refractive indices of the material at the frequency $\omega_{L,S}$ of the incident (scattered) laser light, $\mathbf{k}_{L,S}$ are the wave vectors of the incident (scattered) light. $M^*=(1/M_{\rm Ga}+1/M_{\rm As})^{-1}$ is the reduced mass of the primitive cell of GaAs (volume $V_c=a_0^3/4$, where a_0 is the lattice constant), $\Omega_{\rm LO}$ the frequency of the LO phonon. V denotes the crystal volume. The most resonant contributions to the transition amplitude can be written in fourth-order perturbation theory:

$$W_{fi}(\mathbf{q},\mathbf{q}')=\sum_{\substack{\mathbf{K},\mathbf{K}',\mathbf{K}'',\\ \mathbf{k},\mathbf{k}',\mathbf{k}''}}\frac{\langle 0|a_{\mathbf{k}_L\hat{e}_L}H_{eR}b^\dagger_{\mathbf{kk}}|0\rangle}{\hbar\omega_L+i\eta-\varepsilon_c(\mathbf{K})-\varepsilon_v(\mathbf{K})}$$
$$\times\left\{\frac{\langle 0|b_{\mathbf{kK}}H_F(\mathbf{q})b^\dagger_{\mathbf{k}'\mathbf{K}'}c^\dagger_{\mathbf{q}}|0\rangle\langle 0|b_{\mathbf{k}'\mathbf{K}'}c_{\mathbf{q}}H_{ei}(\mathbf{q}')b^\dagger_{\mathbf{k}''\mathbf{K}''}c^\dagger_{\mathbf{q}}|0\rangle\langle 0|b_{\mathbf{k}''\mathbf{K}''}c_{\mathbf{q}}H_{eR}c^\dagger_{\mathbf{q}}a^\dagger_{\mathbf{k}_S\hat{e}_S}|0\rangle}{[\hbar\omega_L+i\eta-\varepsilon_c(\mathbf{K}')-\varepsilon_v(\mathbf{K}')-\hbar\Omega_{\rm LO}][\hbar\omega_L+i\eta-\varepsilon_c(\mathbf{K}'')-\varepsilon_v(\mathbf{K}'')-\hbar\Omega_{\rm LO}]}\right.$$
$$\left.+\frac{\langle 0|b_{\mathbf{kK}}H_{ei}(\mathbf{q})b^\dagger_{\mathbf{k}'\mathbf{K}'}|0\rangle\langle 0|b_{\mathbf{k}'\mathbf{K}'}H_F(\mathbf{q}')b^\dagger_{\mathbf{k}''\mathbf{K}''}c^\dagger_{\mathbf{q}}|0\rangle\langle 0|b_{\mathbf{k}''\mathbf{K}''}c_{\mathbf{q}}H_{eR}c^\dagger_{\mathbf{q}}a^\dagger_{\mathbf{k}_S\hat{e}_S}|0\rangle}{[\hbar\omega_L+i\eta-\varepsilon_c(\mathbf{K}')-\varepsilon_v(\mathbf{K}')][\hbar\omega_L+i\eta-\varepsilon_c(\mathbf{K}'')-\varepsilon_v(\mathbf{K}'')-\hbar\Omega_{\rm LO}]}\right\}. \tag{3}$$

H_{eR} is the electron- (hole-) photon interaction and $H_F(\mathbf{q})$ the Fröhlich interaction between an electron-hole pair and a LO phonon with pseudomomentum $\hbar\mathbf{q}$. $a^\dagger_{\mathbf{k}\hat{e}}$, $b^\dagger_{\mathbf{kK}}$, and $c^\dagger_{\mathbf{q}}$ are creation operators for a photon with momentum $\hbar\mathbf{k}$ and a polarization $\hat{e}$, an electron-hole (e-h) pair with total pseudomomentum $\hbar\mathbf{k}(\mathbf{k}=\mathbf{k}_e-\mathbf{k}_h)$ and relative pseudomomentum $\hbar\mathbf{K}(\mathbf{K}=s_e\mathbf{k}_e+s_h\mathbf{k}_h)$, and a LO phonon with pseudomomentum $\hbar\mathbf{q}(\mathbf{q}=\mathbf{k}_L-\mathbf{k}_S)$, respectively. Using only a two-band model, consisting of the $n=2$, conduction and the $n=2$, heavy-hole band, the quantities $s_{e,h}$ are defined by

$$s_e=m_{e\perp}/m,\quad s_h=m_{h\perp}/m,\quad m=m_{e\perp}+m_{h\perp}\,. \tag{4}$$

$m_{e,h\perp}$ are the conduction-electron, heavy-hole effective masses in the direction parallel to the layer (perpendicular to the nondispersive axis), respectively. In Eq. (3), $H_{ei}(\mathbf{q})$ denotes the electron- (hole-) impurity interaction via a screened Coulomb potential yielding a momentum transfer $\hbar\mathbf{q}$. In the effective mass approximation for two bands the transition energy becomes

$$\varepsilon_c(\mathbf{K})-\varepsilon_v(\mathbf{K})=E(n=2,\mathrm{HH})+\frac{\hbar^2}{2\mu_\perp}K_\perp^2\,. \tag{5}$$

$E(n=2,\mathrm{HH})$ is the energy of the $n=2$, heavy-hole exciton transition, $\hbar K_\perp$ the relative pseudomomentum of electron and hole parallel to the layer (perpendicular to the nondispersive axis), and $\mu_\perp$ the reduced exciton mass [$\mu_\perp=(1/m_{e\perp}+1/m_{h\perp})^{-1}$].

The electron-photon interaction yields the matrix element

$$\langle 0 \mid a_{\mathbf{k}\hat{e}} H_{eR} b^{\dagger}_{\mathbf{k}'\mathbf{K}} \mid 0 \rangle = \frac{e}{m} \left[\frac{4\pi}{Vn^2} \right]^{1/2} \left[\frac{\hbar}{2\omega} \right]^{1/2} \times \langle c \mid \mathbf{p}\cdot\hat{e} \mid v \rangle \delta_{\mathbf{k},\mathbf{k}'} , \quad (6)$$

where e (m) are the free-electron charge (mass), n is the refractive index of the material at the frequency ω, and $\langle c \mid \mathbf{p}\cdot\hat{e} \mid v \rangle$ denotes the momentum matrix element between the valence-band and conduction-band state for the polarization $\hat{e}$ of $\mathbf{p}$. Including spin degeneracy we chose $\mid \langle c \mid \mathbf{p}\cdot\hat{e} \mid v \rangle \mid^2 = P^2$ as in the case of HH-conduction-band transitions in bulk material.[24] The Fröhlich constant C_F is defined as

$$C_F = [2\pi e^2 (1/\epsilon_\infty - 1/\epsilon_0)\hbar\Omega_{\mathrm{LO}}]^{1/2} , \quad (7)$$

where ϵ_0 and ϵ_∞ denote the low- (rf) and high-frequency (ir) dielectric constant. The matrix element for the Fröhlich interaction then becomes

$$\langle 0 \mid b_{\mathbf{k}\mathbf{K}} H_F(\mathbf{q}) b^{\dagger}_{\mathbf{k}'\mathbf{K}'} c^{\dagger}_{\mathbf{q}} \mid 0 \rangle = i \frac{1}{q} \frac{C_F}{(V)^{1/2}} (\delta_{\mathbf{K},s_e\mathbf{q}+\mathbf{K}'} - \delta_{\mathbf{K}+s_h\mathbf{q},\mathbf{K}'}) \delta_{\mathbf{k},\mathbf{k}'+\mathbf{q}} . \quad (8)$$

We shall take for H_{ei} the screened Coulomb potential of a charge in a 2D electron gas which differs from that in a 3D gas.[25] The electrons are bound in the direction perpendicular to the layer whereas they are free in the two other dimensions. Image potentials at the interfaces have to be accounted for in addition to the polarization of the dielectric. There are two different approaches for the screening of a Coulomb potential by a 2D electron gas. The first one considers strictly 2D sheets of charges,[26] whereas the second attempt deals with a quasi-2D electron gas in a dielectric.[27] Both cases yield complicated expressions for the screened Coulomb potential. The most appropriate one for our purpose of an unintentionally doped quantum well is the quasi-2D approach by Bechstedt and Enderlein.[27] Their final expression includes the polarization of the medium by the impurity as well as the image charges created at the interfaces. For the case of weak screening ($q_F^{-1} \gg d_1/\pi$, q_F is the screening wave vector, $d_1 = 104$ Å is the thickness of the GaAs layer) their results justify the use of a similar expression as in the 3D case. The Fourier transform of the screened potential is thus assumed to be of the form

$$V_s(\mathbf{q}) = \frac{4\pi e^2}{(q_\perp^2 + q_\parallel^2 + q_F^2)\epsilon_0 V} e^{i\mathbf{q}\cdot\mathbf{r}} . \quad (9)$$

Here $q_\perp$ ($q_\parallel$) denotes the wave vector parallel (perpendicular) to the superlattice layer, which signifies perpendicular (parallel) to the nondispersive axis. ϵ_0 is the low-frequency dielectric constant. We shall approximate the screening wave vector q_F by one-half of the distance between impurities [$q_F = 2/\lambda = 2(4\pi n_I/3)^{1/3}$], an approximation which would represent screening by compensated impurities but also should not be too bad in the case of screening by ionized impurities. The matrix element for the electron-impurity interaction then becomes

$$\langle 0 \mid b_{\mathbf{k}\mathbf{K}} H_{ei}(\mathbf{q}) b^{\dagger}_{\mathbf{k}'\mathbf{K}'} \mid 0 \rangle = \frac{4\pi e^2}{(q^2 + q_F^2)\epsilon_0 V} (\delta_{\mathbf{K},s_e\mathbf{q}+\mathbf{K}'} - \delta_{\mathbf{K}+s_h\mathbf{q},\mathbf{K}'}) \delta_{\mathbf{k},\mathbf{k}'+\mathbf{q}} . \quad (10)$$

We neglect $\mathbf{k}_S = \mathbf{k}_L \simeq 0$. Thus, the sums over the $\mathbf{k}$ ($\mathbf{K}$) vectors are trivial in Eq. (3) except that over $\mathbf{K}$. Details of the calculation are carried out in the Appendix. The result for the transition amplitude $W_{fi}(\mathbf{q}, -\mathbf{q})$ [Eq. (3)] can be summarized as follows:

$$W_{fi}(\mathbf{q}, -\mathbf{q}) = 2\pi \left[\frac{e^2}{m} \right] \frac{1}{n_L n_S} \frac{1}{(\omega_L \omega_S)^{1/2}} \frac{\hbar C_F P^2}{V^{3/2}\epsilon_0} \frac{1}{(a^*)^2 d} \times \frac{1}{(\hbar\Omega_{\mathrm{LO}})^3} \frac{1}{q(q^2 + q_F^2)} X(a^* q_\perp) , \quad (11)$$

where d is the length of one superlattice period ($d = d_1 + d_2$). The function $X(a^* q_\perp)$ is defined in the Appendix. It depends on $\mathbf{q}$ only through the component parallel to the superlattice layer while $a^* = (\hbar/2\mu_\perp\Omega_{\mathrm{LO}})^{1/2}$ is a characteristic length. After carrying out the integration over $\mathbf{q}$ vectors in Eq. (2) with cylindrical coordinates one obtains the final result for the squared Raman polarizability:

$$\mid b_{\mathrm{Fi}} \mid^2 = \frac{1}{(2\pi)^2} n_I \left[\frac{e^2}{m} \right]^4 \left[\frac{2M^*\Omega_{\mathrm{LO}} a_0^3}{\hbar} \right] \times \frac{1}{\omega_L^3 \omega_S} \frac{C_F^2 P^4}{\epsilon_0^2} \frac{1}{(a^*)^4 d^2} \frac{1}{(\hbar\Omega_{\mathrm{LO}})^6} \times \int_0^\infty dq_\perp \, q_\perp A(q_\perp) \mid X(a^* q_\perp) \mid^2 . \quad (12)$$

The integral in Eq. (12) can be computed numerically. The weighting function $A(q_\perp)$, defined in Eq. (A7) of the Appendix, results from the integration over $q_\parallel$. Equation (12), together with Eqs. (A2)–(A5) and (A7) of the Appendix, gives the squared Raman polarizability $\mid b_{\mathrm{Fi}} \mid^2$ as a function of the laser energy $\hbar\omega_L$. The expression is a very sensitive function of the screening wave vector q_F. In order to demonstrate the sensitivity of Eq. (12) to the screening wave vector q_F, we evaluated the squared Raman polarizability $\mid b_{\mathrm{Fi}} \mid^2$ for different screenings and reasonable structure parameters of the multiple quantum well, as given by Table I. The results of calculations for $q_F = 0.005$, 0.0125, and 0.02 Å^{-1} are shown in Fig. 2. The screenings correspond, respectively, to the impurity concentration $n_I = 3.7\times10^{15}$ cm^{-3}, 5.8×10^{16} cm^{-3}, and 2.4×10^{17} cm^{-3}, calculated from the mean distance λ between two impurities.

For all screening wave vectors two distinct peaks are seen at the incoming and the outgoing resonance, separated by exactly one phonon energy. The resonance occurs at slightly higher energy than estimated from the e-HH exciton transition. In the 3D case, no separate peaks are observed at incoming and outgoing resonance for comparable broadening of the electronic transition ($\eta = 8$ meV, Fig. 2 of Ref. 18): the resonance curve only exhibits a peak for $\hbar\omega_S$ equal to the gap (outgoing resonance). This

TABLE I. Parameters used for the evaluation of the squared Raman polarizability $|b_{FI}|^2$.

E $(n=2,\mathrm{HH})$	1.642 eV[a]
η	7 meV[a]
$\hbar\Omega_{LO}$	38 meV[b]
$m_{e\perp}$	0.067 m[c]
$m_{h\perp}$	0.34 m[c]
a^*	43.2 Å[c]
P^2/m	12.9 eV[c]
C_F	2.14×10^{-5} eV cm$^{1/2}$[c]
ϵ_0	13.1[c]
a_0	5.65 Å[c]
M^*	66285.6 m[c]

[a]Determined from the fit of the experimental data.
[b]In order to account for the peak separation between the incoming and outgoing resonance, the phonon energy has to be slightly increased (see Ref. 2 and text).
[c]Chosen as for bulk GaAs.

difference results from the divergence of the Green's function for uncorrelated pairs (logarithmic singularity) at a two-dimensional electronic transition. No such divergence occurs in the three-dimensional case. The asymmetry of the incoming and outgoing resonance amounts to about 1, 2, and 2.8 for $q_F=0.005$, 0.0125, and 0.02 Å^{-1}, respectively. It depends sensitively on the screening wave vector. The scattered intensity decreases as the screening increases.

B. Comparison with experiment

In order to compare the result of our calculation with the experimental ones near the $n=2$, e-HH exciton in Fig. 1, we corrected the scattering rates *outside* the crystal for reflectivity, absorption, and refractive index. For opaque materials the relation between the counting rate

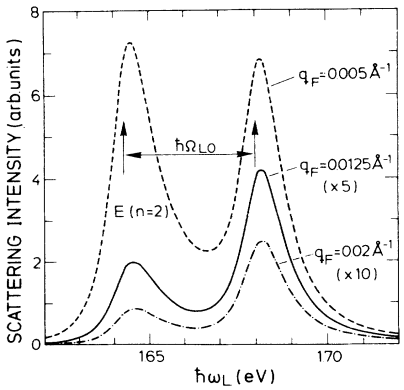

FIG. 2. Resonance of the impurity-induced Fröhlich scattering by LO phonons at a quasi-two-dimensional exciton transition. The calculations [Eqs. (12) with (A2)–(A5) and (A7)] were performed for the parameters of Table I and with different screening wave vectors q_F. The vertical scale represents scattering intensities in arbitrary units which differ, in the three curves, by the following factors: the curve for $q_F=0.0125$ Å^{-1} has been multiplied by 5, that for $q_F=0.02$ Å^{-1} by 10.

R_s' *outside* the crystal and the squared Raman polarizability (*inside* the crystal) $|\hat{e}_S\cdot\vec{\mathbf{R}}\cdot\hat{e}_L|^2$ is given by[19]

$$R_s'=\left[\frac{T_S T_L \omega_S^3[n(\Omega_{Ph})+1]}{(\alpha_L+\alpha_S)n_S n_L M^*\Omega_{Ph}V_c}\right]\frac{P_L'\Delta\Omega'}{2c^4}\,|\hat{e}_S\cdot\vec{\mathbf{R}}\cdot\hat{e}_L|^2\,. \tag{13}$$

In Eq. (13) P_L' is the incident laser power and $\Delta\Omega'$ is the solid angle of collection *outside* the crystal while $n(\Omega_{Ph})$ denotes the phonon occupation number. $T_{L,S}$, $\alpha_{L,S}$, and $n_{L,S}$ are the power-transmission coefficient, the absorption coefficient, and the refractive index at the frequency of the incident (scattered) light, respectively. To convert the measured counting rates *outside* the crystal into absolute squared Raman polarizabilities *inside* the crystal the large bracket in Eq. (13) has to be applied as a correction factor for the multiple-quantum-well (MQW) sample and silicon reference. For Si, we used the absorption data of Dash and Newman,[28] and $|a_{Si}|=30$ Å^2 at 1.65 eV.[29] For the multiple quantum well studied no absorption data were available. For different GaAs/$Ga_{1-x}Al_xAs$ MQW absorption measurements have been published covering the $n=1-4$ exciton region.[8,9,30–32] The definition of an absorption coefficient in the direction perpendicular to the layer must require an averaging because of the inhomogeneous nature of a superlattice. It is natural to define it as

$$\alpha=\frac{1}{nd}\sum_{i=1}^{n}\ln\left[\frac{\Delta I}{I}\right]_i=\frac{1}{nd}\ln\left[\frac{\Delta I}{I}\right], \tag{14}$$

where n is the number of periods of the superlattice ($=100$) and d the thickness of one period ($d_1+d_2=229$ Å). $(\Delta I/I)_i$ is the relative decrease in intensity occurring in one period whereas $\Delta I/I$ denotes the relative decrease in intensity for the total superlattice. An absolute measurement of the absorption coefficient can be found in Ref. 32 for a multiple quantum well 102 Å GaAs/207 Å $Ga_{0.72}Al_{0.28}As$ at room temperature in the region below the $n=2$ exciton. Relative absorption data for a 116 Å GaAs/200 Å $Ga_{0.75}Al_{0.25}As$ multiple quantum well across the $n=2$ region are published in Ref. 9 by Gossard.

Using Eq. (14) and scaling the data of Miller[32] and Gossard[9] in the region between the $n=1$ and $n=2$ exciton we calibrated in cm^{-1} the absorption scale (given in arbitrary units in Fig. 15 of Ref. 9). The photon energy scale was shifted by 12 meV to account for the different $n=2$, HH-exciton energies (Gossard's 1.63 eV, ours 1.642 eV). Uncertainties in this correction should introduce an error of about 50% in the value of the absolute squared Raman polarizability. It should correct, however, reasonably well for the steplike increase in absorption in the region of the $n=2$ exciton[7] and thus slightly modify the asymmetry of the incoming and outgoing resonances near the $n=2$ e-HH exciton (Fig. 1). The corrected data near the $n=2$, e-HH exciton resonance are presented as dots in Fig. 3. The solid line is a fit with Eq. (12) using the parameters of Table I and $q_F=0.0125$ Å^{-1}. From the width and the position of the resonance we determine the broadening and the position of the $n=2$, HH-exciton transition to be

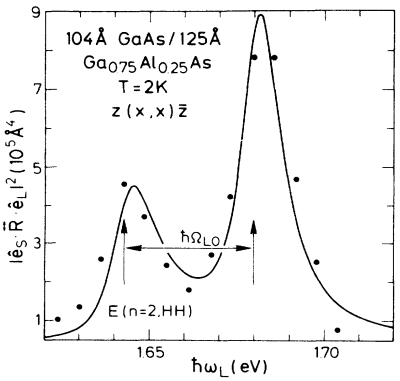

FIG. 3. Comparison of the experimental data, corrected for absorption as described in the text (closed circles), with the calculation (solid line) near the resonance at the $n=2$ electron–heavy-hole exciton. The theoretical curve has been raised by 5×10^4 Å^4 to account for a nonresonant contribution. The parameters of the calculation were taken from Table I and q_F chosen to be 0.0125 Å^{-1}.

7 meV and 1.642 eV, respectively. The broadening is larger than obtained from absorption for the $n=1$ exciton ($\eta=2$ meV).[32] The measured broadening may include a contribution from the roughness of the interface (about four times larger for $n=2$ than for $n=1$) and, in any case, an $n=2$ exciton is expected to have a larger broadening than for $n=1$ because of the additional available decay channels.

As already pointed out by Zucker *et al.*,[2] the energy of the LO phonon has to be chosen slightly higher (38 meV instead of 36.6 meV) to account for the energy separation of the resonance peaks. A possibly similar renormalization of LO-phonon energies has been also reported for conduction-band-acceptor transitions seen in the hot luminescence of *p*-type GaAs.[33] The comparison of the absolute squared Raman polarizabilities obtained experimentally and those calculated with Eq. (12) for the resonant part of the forbidden scattering by LO phonons using the parameters of Table I yields an experimental value about 11 times larger than the theoretical one for $n_I=5.8\times10^{16}$ cm^{-3} ($q_F=0.0125$ Å^{-1}). This order of magnitude agreement is acceptable in view of the simplified nature of the model, in particular of the defect potential. The theory considers only the most resonant terms and neglects the correlation of electron-hole pairs (excitons). The screening of the Coulomb potential, which is known to be quite different in the pure two-dimensional limit, may also have a large influence on the quantitative results.

Zucker *et al.*[2,14] explain the asymmetry of incoming and outgoing resonances by assuming that the phonon couples excitons associated with different subbands. Coupling to a lower exciton state (intermediate state) should yield stronger incoming resonances while the opposite should apply if this exciton is higher than the resonating one. The main problem with such a model is that, in order to have optically allowed transitions, it requires strong coupling of subbands by the excitonic interaction. While this may happen under special circumstances,[14] it will not hold in general.

The impurity-induced intraband Fröhlich Raman scattering proposed in this paper should be generally valid provided the screening wave vector stays below the length of the mini-Brillouin-zone and the screened Coulomb potential can be assumed to be a constant over the envelope function of the exciton states under resonance. A removal of both restrictions is possible, in principle, including a screened Coulomb potential, such as presented in Ref. 27, as well as the detailed exciton wave functions. However, the integrals in **K** and **q** space must then be computed numerically, thus losing the simplicity of our analytic expressions. An extension of this theory may also be able to explain stronger incoming (or still stronger outgoing) resonances than, e.g., observed for the $n=2$, heavy-hole exciton in the GaAs (104 Å)/ $Ga_{0.75}Al_{0.25}As$ (125 Å) superlattice.[2,14] The model presented above has the advantage that it does not depend on the specific nature of the intermediate electronic states, except for the assumption of uncorrelated electron-hole pairs. In the case of resonant Raman scattering by LO phonons with extended exciton states, not only the variation of the Coulomb potential over the exciton envelope function may be considerable, but also the scattering due to the roughness of the interface, which can provide any **q** vector, should be taken into account.

IV. CONCLUSION

We have shown that intraband impurity-induced forbidden scattering by LO phonons can explain the observed asymmetry in the $n=2$, *e*-HH-exciton resonance. The exact position as well as the broadening of the $n=2$ exciton transition are obtained from a theoretical fit. This fit gives also an estimate of the ionized-impurity concentration or an equivalent defect concentration. We believe that the scattering mechanism proposed, and the theory developed, should be generally valid as long as the screening wave vector stays below the length of the mini-Brillouin-zone.

ACKNOWLEDGMENTS

The authors are indebted to H. Hirt, M. Siemers, and P. Wurster for their technical assistance.

APPENDIX

In order to carry out the sum over the electronic density of states in Eq. (3) for the quasi-two-dimensional case, one has to transform the sum $\sum_{\mathbf{K}}$ into an integral in cylindrical coordinates:

$$\frac{V}{(2\pi)^3}\int d^3K=\frac{V}{(2\pi)^3}\int_{-\pi/d}^{+\pi/d}dK_{\parallel}\int_0^{2\pi}d\phi_K\int_0^{\infty}K_{\perp}\,dK_{\perp}$$
$$=\frac{V}{2\pi d}\int K_{\perp}\,dK_{\perp}\,, \tag{A1}$$

where d is the length of one superlattice period. We have assumed that the Coulomb potential is constant over the envelope functions of the $n=2$, electron and hole states, an assumption justified by the condition $q_F^{-1} \gg d_1/\pi$ (d_1 is the thickness of the GaAs layer).

After the decomposition of the denominators in Eq. (3) into partial fractions, the $K_\perp$ integration leads to the standard form of integral[34,35]:

$$I(-A,B,C)=\int_0^\infty \frac{1}{(x-A)(x^2+2Bx+C^2)^{1/2}}dx = \frac{1}{(z)^{1/2}}\ln\left[\frac{(z)^{1/2}C-C^2-AB}{A(z^{1/2}+A+B)}\right], \quad \text{(A2)}$$

with $z=A^2+2AB+C^2$ and $x=(a^*)^2K_\perp^2$.

The integration over $K_\perp$ in Eqs. (3) and (A1) yields the function $X(a^*q_\perp)$ of Eq. (11), with $X(a^*q_\perp)$ defined as

$$\begin{aligned}X(a^*q_\perp)=&I(-\alpha,a,b)-I(-\beta,a,b)+I(-\alpha,g,h)-I(-\beta,g,h)+I(-\alpha,c,d)-I(-\beta,c,d)+I(-\alpha,i,j)-I(-\beta,i,j)\\&+\frac{1}{s_h-s_es_h(a^*)^2q_\perp^2}[s_eI(-\alpha,a,b)-s_eI(-\delta',a,b)-I(-\alpha,k,l)+I(-\delta',k,l)]\\&-\frac{1}{s_e+s_es_h(a^*)^2q_\perp^2}[s_eI(-\alpha,g,h)-s_eI(-\delta'',g,h)-I(-\alpha,k,l)+I(-\delta'',k,l)]\\&+\frac{1}{s_e-s_es_h(a^*)^2q_\perp^2}[s_hI(-\alpha,c,d)-s_hI(-\varepsilon',c,d)-I(-\alpha,k,l)+I(-\varepsilon',k,l)]\\&-\frac{1}{s_h+s_es_h(a^*)^2q_\perp^2}[s_hI(-\alpha,i,j)-s_hI(-\varepsilon'',i,j)-I(-\alpha,k,l)+I(-\varepsilon'',k,l)]\ . \quad \text{(A3)}\end{aligned}$$

$X(a^*q_\perp)$ depends on functions of the laser energy through the dimensionless quantities α and β defined as[21]

$$\alpha=[\hbar\omega_L+i\eta-E(n=2,\mathrm{HH})]/\hbar\Omega_{\mathrm{LO}},\quad \beta=\alpha-1\ , \quad \text{(A4)}$$

where η is the broadening of the $n=2$, e-HH exciton level. The variables introduced in (A3) are defined as follows:

$$\begin{aligned}&a=-\beta-(a^*)^2s_e^2q_\perp^2,\quad b=a+2\beta\ ,\\&c=-\beta-(a^*)^2s_h^2q_\perp^2,\quad d=c+2\beta\ ,\\&g=-\alpha-(a^*)^2s_e^2q_\perp^2,\quad h=g+2\alpha\ ,\\&i=-\alpha-(a^*)^2s_h^2q_\perp^2,\quad j=i+2\alpha\ ,\\&k=-\beta-(a^*)^2q_\perp^2,\quad l=k+2\beta\ ,\\&\delta'=\beta+s_e(a^*)^2q_\perp^2,\quad \delta''=\alpha+\frac{s_e}{s_h}+s_e(a^*)^2q_\perp^2\ ,\\&\varepsilon'=\beta+s_h(a^*)^2q_\perp^2,\quad \varepsilon''=\alpha+\frac{s_h}{s_e}+s_h(a^*)^2q_\perp^2\ .\end{aligned} \quad \text{(A5)}$$

The sum over the phonon branch $[\mathbf{q}=(q_\parallel,q_\perp)]$ must also be carried out in cylindrical coordinates whereby we neglect the dispersion of the LO-phonon energy. The angular integration yields the factor 2π, whereas the integration of $q_\parallel$ over the whole length of the Brillouin zone gives

$$\int_{-2\pi/a_0}^{+2\pi/a_0} dq_\parallel \frac{1}{(q_\parallel^2+q_\perp^2)(q_\parallel^2+q_\perp^2+q_F^2)^2}=A(q_\perp)\ , \quad \text{(A6)}$$

with $A(q_\perp)$ defined as[34]

$$\begin{aligned}A(q_\perp)=&\frac{6\pi/a_0}{q_F^2(q_\perp^2+q_\parallel^2)(4\pi^2/a_0^2+q_\perp^2+q_F^2)}\\&-\frac{1}{q_F''}\frac{(2q_\perp^2-q_F^2)}{(q_\perp^2+q_F^2)^{3/2}}\arctan\left[\frac{2\pi/a_0}{(q_\perp^2+q_F^2)^{1/2}}\right]\\&+\frac{2}{q_F^4}\frac{1}{q_\perp}\arctan\left[\frac{2\pi/a_0}{q_\perp}\right]\ . \quad \text{(A7)}\end{aligned}$$

The integration in Eq. (A6) replaces the sum over the discrete confined modes. This is justifiable for large period superlattices. The limits of integration in Eq. (A6) can be set equal to infinity without any loss in accuracy. The squared Raman polarizability thus reduces to Eq. (12) which is integrated numerically.

*Present address: Materials Science Laboratory, Indira Gandhi Centre for Atomic Research, Kalpakkam 603 102, Tamil Nadu, India.

[1]M. V. Klein, IEEE J. of Quantum Electron. **22**, 1760 (1986).
[2]J. E. Zucker, A. Pinczuk, D. S. Chemla, A. Gossard, and W. Wiegmann, Phys. Rev. Lett. **51**, 1293 (1983).
[3]E. E. Mendez, L. L. Chang, G. Landgren, R. Ludeke, and L. Esaki, Phys. Rev. Lett. **46**, 1230 (1981).
[4]R. C. Miller, D. A. Kleinman, W. A. Nordland, Jr., and A. C. Gossard, Phys. Rev. B **22**, 863 (1980).
[5]R. C. Miller, D. A. Kleinman, W. T. Tsang, and A. C. Gossard, Phys. Rev. B **24**, 1134 (1981).
[6]G. Bastard, Phy. Rev. B **24**, 5693 (1981).
[7]R. Dingle, in *Confined Carrier Quantum States in Ultrathin Semiconductor Heterostructures* in *Festkörperprobleme XV*, edited by H.-J Queisser (Pergamon-Vieweg, Braunschweig, 1975), p. 21.
[8]D. S. Chemla, Hel. Phys. Acta **56**, 607 (1983).
[9]A. C. Gossard, in *Molecular Beam Epitaxy of Superlattices in Thin Films*, in *Treatise on Materials Science and Technology*,

Vol. 24, edited by K. N. Tu and R. Rosenberg (Academic, New York, 1983).
[10]A. K. Sood, J. Menéndez, M. Cardona, and K. Ploog, Phys. Rev. Lett. **54**, 2111 (1985).
[11]A. S. Barker, Jr., J. L. Merz, and A. C. Gossard, Phys. Rev. B **17**, 3181 (1978).
[12]B. Jusserand, D. Paquet, and A. Regreny, Phys. Rev. B **30**, 6245 (1984).
[13]P. Manuel, G. A. Sai-Halasz, L. L. Chang, C.-A. Chang, and L. Esaki, Phys. Rev. Lett. **37**, 1701 (1976).
[14]J. E. Zucker, A. Pinczuk, D. S. Chemla, A. Gossard, and W. Wiegmann, Phys. Rev. B **29**, 7065 (1984).
[15]T. Suemoto, G. Fasol, and K. Ploog, in *Proceedings of the Eigtheenth International Conference on the Physics of Semiconductors*, Stockholm, 1986, edited by O. Engström (World Scientific, Singapore, 1987), p. 683.
[16]T. Suemoto, G. Fasol, and K. Ploog, Phys. Rev. B **34**, 6034 (1986).
[17]For a discussion of the three-dimensional case, see R. M. Martin, Phys. Rev. B **4**, 3676 (1971); R. Zeyher, C.-S. Ting, and J. L. Birman, Phys. Rev. B **10**, 1725 (1974).
[18]W. Kauschke and M. Cardona, Phys. Rev. B **33**, 5473 (1986).
[19]J. Menéndez and M. Cardona, Phys. Rev. B **31**, 3696 (1985).
[20]G. A. Sai-Halasz, A. Pinczuk, P. Y. Yu, and L. Esaki, Solid State Commun. **25**, 381 (1978).
[21]W. Richter, R. Zeyher, and M. Cardona, Phys. Rev. B **18**, 4312 (1978).
[22]For formalism see also, R. Zeyher, Phys. Rev. B **9**, 4439 (1974).
[23]J. Menéndez, Ph.D. thesis, Universität Stuttgart, 1985.
[24]M. Cardona, in *Light Scattering in Solids II*, Vol. 50 of *Topics in Applied Physics*, edited by M. Cardona and G. Güntherodt, (Springer, Heidelberg, 1982), p. 19.
[25]J. Lee and H. N. Spector, J. Appl. Phys. **54**, 6989 (1983).
[26]F. Stern and W. E. Howard, Phys. Rev. **163**, 816 (1967).
[27]F. Bechstedt and R. Enderlein, Phys. Status Solidi B **131**, 53 (1985).
[28]W. C. Dash and R. Newman, Phys. Rev. **99**, 1151 (1955).
[29]J. Wagner and M. Cardona, Solid State Commun. **48**, 301 (1983).
[30]R. Dingle, W. Wiegmann, and C. H. Henry, Phys. Rev. Lett. **33**, 827 (1974).
[31]R. Dingle, A. C. Gossard, and W. Wiegmann, Phys. Rev. Lett. **34**, 1327 (1975).
[32]D. A. B. Miller, D. S. Chemla, D. J. Eilenberger, P. W. Smith, A. C. Gossard, and W. T. Tsang, Appl. Phys. Lett. **41**, 679 (1982).
[33]G. Fasol, K. Ploog, and E. Bauser, Solid State Commun. **54**, 383 (1985).
[34]I. S. Gradshteyn and I. M. Ryzhik, *Table of Integrals, Series, and Products* (Academic, New York, 1965).
[35]M. A. Renucci, J. B. Renucci, R. Zeyher, and M. Cardona, Phys. Rev. B **10**, 4309 (1974).